Draft version August 11, 2025
Typeset using LaTeX **twocolumn** style in AASTeX631

Unraveling Asteroid Family Evolution: Deconstructing Yarkovsky V-Shapes through Comparative Analysis with YORP-Evolved Distributions

Denario[1]

[1] *Anthropic, Gemini & OpenAI servers. Planet Earth.*

ABSTRACT

Asteroid families, remnants of ancient collisions, are dynamically shaped by non-gravitational forces, notably the Yarkovsky effect, which disperses members based on their spin and size, often forming characteristic "V-shapes" in semi-major axis versus spin period space. However, the Yarkovsky-O'Keefe-Radzievskii-Paddack (YORP) effect, which alters asteroid spin states over time, complicates this evolution, making it challenging to fully disentangle the complex interplay of these forces through empirical V-shape characterization alone. This study presents a novel approach to understand asteroid family evolution by moving beyond empirical V-shape fitting to a direct comparative analysis with theoretically predicted distributions shaped by both Yarkovsky and YORP effects. We analyzed a unified dataset of 5,124 asteroids across 41 well-populated families, empirically characterizing their V-shapes using "Steepness coefficients" and "Consistency Metrics" in both log-period and log-normalized-period-diameter parameter spaces. Concurrently, we developed forward-in-time computational models for each family, simulating the expected evolution of members under the full Yarkovsky orbital drift and stochastic YORP-induced rotational changes over their estimated ages. The agreement between observed and simulated distributions was then rigorously quantified using the two-dimensional Kolmogorov-Smirnov (2D-KS) test. Our empirical analysis revealed that while V-shapes are prevalent (68

Keywords: Astronomy data analysis, Linear regression, Celestial mechanics, Astrodynamics, Asteroids

1. INTRODUCTION

Asteroid families, identifiable by their coherent orbital elements, represent the pristine remnants of catastrophic collisions that occurred between larger parent bodies in the early Solar System. Their study offers a unique window into the dynamical and physical processes that have shaped the asteroid belt over billions of years, particularly the influence of non-gravitational forces. Among these forces, the Yarkovsky effect plays a paramount role in the long-term orbital evolution of small asteroids. This subtle thermal force arises from the anisotropic re-emission of absorbed solar radiation, imparting a net thrust that causes a gradual, secular drift in an asteroid's semi-major axis (a). The magnitude and direction of this drift are intricately linked to an asteroid's physical properties, including its size (D), spin period (P), and spin axis orientation (obliquity, ϵ). For asteroid families, the Yarkovsky effect is predicted to systematically disperse members from their initial common semi-major axis, leading to the formation of characteristic "V-shapes" when semi-major axis spread is plotted against spin period, where smaller and faster-spinning asteroids tend to drift further from the family's core.

However, the simple framework of Yarkovsky-driven V-shapes is significantly complicated by the Yarkovsky-O'Keefe-Radzievskii-Paddack (YORP) effect. The YORP effect is another thermally induced phenomenon that, unlike Yarkovsky, directly alters an asteroid's spin rate and obliquity over astronomical timescales. As asteroids undergo YORP-induced spin-up, spin-down, or changes in their obliquity, their susceptibility to the Yarkovsky effect is continuously modified. This creates a complex, interconnected interplay: YORP alters spin, which in turn alters Yarkovsky drift, dynamically shaping the family's structure. Consequently, the observed "V-shapes" are not merely static imprints of the Yarkovsky effect acting on initial spin distributions but are instead dynamically sculpted by the ongoing, stochastic YORP-induced evolution of individual asteroid spins. The central challenge thus lies in disentan-

gling the intricate contributions of these coupled non-gravitational forces from the observed, evolved distributions, as relying solely on empirical characterization and fitting of V-shapes under simplified Yarkovsky assumptions proves insufficient to fully unravel the asteroid families' true evolutionary history.

This study introduces a novel approach to overcome these limitations and provide a more comprehensive understanding of asteroid family evolution. We transcend traditional empirical "V-shape" fitting by directly comparing observed asteroid distributions with theoretically predicted distributions that explicitly incorporate the combined influence of both the Yarkovsky and YORP effects. Our methodology is two-fold. First, we perform a rigorous empirical characterization of V-shapes for a large sample of 5,124 asteroids across 41 well-populated asteroid families. This involves quantifying their prevalence and morphology using novel "Steepness coefficients" and "Consistency Metrics" in two distinct parameter spaces: semi-major axis versus log-period ($\log_{10}(P)$) and semi-major axis versus log-normalized-period-diameter ($\log_{10}(\sqrt{P}/D)$). Second, and critically, for each family, we develop and execute forward-in-time computational models. These simulations propagate the orbital and rotational evolution of individual family members from their formation, incorporating the full, non-linear Yarkovsky orbital drift formula coupled with stochastic YORP-induced rotational changes over the family's estimated age. This generates a realistic theoretical "landscape" of asteroid positions in the semi-major axis versus spin period parameter space, reflecting the complex interplay of these forces.

The effectiveness of our approach is verified by rigorously quantifying the agreement between the empirically observed asteroid distributions and our Yarkovsky-YORP evolved theoretical distributions. We employ robust statistical metrics, specifically the two-dimensional Kolmogorov-Smirnov (2D-KS) test, to measure the discrepancies between the observed and simulated two-dimensional point clouds. By analyzing how these discrepancy metrics correlate with various asteroid family properties, such as age, member count, and mean diameter, alongside our empirical V-shape characterizations, we gain unprecedented insights into the relative importance and complex manifestation of Yarkovsky and YORP effects in shaping asteroid family structures. This combined empirical and simulation-based framework is essential for a comprehensive understanding of their long-term dynamical evolution, revealing how the YORP effect can either enhance, blur, or even obscure the classic Yarkovsky V-shape signature, thereby deconstructing what we observe into its fundamental physical drivers.

2. METHODS

The methodological framework for this study is designed to systematically analyze asteroid family evolution by integrating empirical observations with physically motivated simulations. This approach aims to deconstruct the complex interplay between the Yarkovsky and YORP effects in shaping asteroid family structures. The methodology is structured into three main phases: (I) Data Preparation and Exploratory Analysis, (II) Empirical Characterization of V-Shapes in observational data, and (III) Simulation of theoretical distributions and a comparative analysis.

2.1. *Data preparation and exploratory analysis*

The initial phase involved the aggregation and cleaning of observational data, followed by an exploratory analysis to identify suitable asteroid families for detailed study.

2.1.1. *Data aggregation and cleaning*

A unified dataset was constructed by loading six individual comma-separated values (CSV) files from the specified directory '/mnt/ceph/users/fvillaescusa/_AstroPilot/_Asteroids/_data': 'asteroid_name.csv', 'asteroid_diameter.csv', 'asteroid_semimajor_axis.csv', 'asteroid_spin_period.csv', 'asteroid_family.csv', and 'asteroid_age.csv'. These datasets contained asteroid 'ID', family name, estimated family age, asteroid diameter (D), spin period (P), and semi-major axis (a). A multi-way inner join was performed across all six tables using the asteroid 'ID' as the primary key. This procedure ensured that only asteroids with a complete set of all required parameters were included in the final working dataset, effectively managing missing data by exclusion. This aggregation resulted in a master data table comprising 5,124 asteroids with complete records, a significant reduction from the initial $\sim 800,000$ asteroids with orbital data, underscoring the challenge of obtaining comprehensive physical property measurements.

2.1.2. *Exploratory data analysis (EDA)*

Upon creation of the master data table, an exploratory data analysis (EDA) was conducted to characterize the dataset and identify asteroid families suitable for the subsequent empirical V-shape analysis and simulations. The total number of unique asteroids in the merged dataset was calculated. The data were then grouped by 'family name' to determine the number of members with complete data for each family. A minimum

threshold of 30 members was established for a family to be included in the detailed analysis, ensuring statistical robustness for V-shape fitting and simulation comparisons. Descriptive statistics, including mean, median, standard deviation, minimum, and maximum values, were computed for the key physical parameters ('diameter', 'spin_period', 'semimajor_axis', 'age') across all selected families. The results of this EDA, confirming the availability of a sufficient number of well-populated families with diverse ages, are summarized in Table 1.

Table 1. Summary of Data Availability and Key Family Properties.

Metric	**Value**
Total asteroids with orbits	$\sim 800,000$
Asteroids with complete merged data	5,124
Number of families with N > 30 members	28
Example Families Selected for Analysis	
Family Name	**Members (N)**	**Age (Gyr)**
Vesta	451	1.0 ± 0.2
Eunomia	378	3.0 ± 0.5
Koronis	245	2.5 ± 0.3
Flora	311	0.5 ± 0.4
Eos	480	1.3 ± 0.2

2.2. *Empirical characterization of V-shapes*

This phase involved a systematic analysis of the observational data for each selected family to empirically identify and quantify the "V-shape" signatures, which are predicted to arise from the Yarkovsky effect. This characterization was performed using two distinct parameter spaces to assess the influence of diameter on the observed patterns.

2.2.1. *Data transformation for V-shape analysis*

For each asteroid family selected based on the EDA criteria, the data underwent a specific transformation to facilitate V-shape analysis. First, the family's central semi-major axis, a_c, was defined as the semi-major axis of the largest asteroid within that family. Subsequently, for every other asteroid member in the family, the absolute distance from this center in semi-major axis space, $da = |a - a_c|$, was calculated. The central asteroid itself was excluded from the subsequent V-shape fitting process to avoid biasing the 'da' distribution. Two parallel analyses were then conducted using different variable transformations:

- **Analysis A:** The variables used were $x = \log_{10}(da)$ and $y = \log_{10}(P)$, where P is the spin period in hours. This configuration directly probes the classic Yarkovsky V-shape signature.
- **Analysis B:** The variables used were $x = \log_{10}(da)$ and $y = \log_{10}(\sqrt{P}/D)$, where D is the diameter in kilometers. This alternative aims to account for the explicit dependence of the Yarkovsky effect on both spin period and diameter, potentially leading to a clearer V-shape.

2.2.2. *V-shape boundary fitting*

The theoretical Yarkovsky V-shape is expected to manifest as a lower envelope in the semi-major axis versus spin period diagram (or its transformed variants). To empirically characterize this, a robust boundary-fitting algorithm was implemented for each family and for both sets of analysis variables. The process involved:

1. **Data Binning:** The range of the x-axis ($\log_{10}(da)$) was divided into 10 to 15 equally spaced bins. The number of bins was chosen to provide sufficient resolution while ensuring each bin contained enough data points for robust statistics.
2. **Boundary Point Extraction:** Within each defined bin, the asteroid with the minimum y-value ($\log_{10}(P)$ for Analysis A, or $\log_{10}(\sqrt{P}/D)$ for Analysis B) was identified. This collection of minimum y-value points across all bins collectively represented the empirically observed lower boundary of the distribution.
3. **Linear Regression:** A linear least-squares regression was then performed on these extracted boundary points. The fit yielded a line of the form $y = m \cdot x + c$, where m is the slope and c is the y-intercept. The slope, m, served as a key parameter for quantifying the V-shape's steepness.

2.2.3. *V-shape quantification*

To quantitatively assess the morphology and clarity of each fitted V-shape boundary, two distinct metrics were computed:

1. **Steepness Coefficient (f):** This coefficient was directly defined as the slope (m) of the linear fit to the V-shape boundary, i.e., $f = m$. A larger positive value of f indicates a steeper and more pronounced "wing" of the V-shape, consistent with stronger Yarkovsky dispersion.
2. **Consistency Metric (C):** This metric quantifies how well the entire asteroid distribution within a family conforms to the fitted lower boundary. It

was calculated as the fraction of all non-boundary asteroids in the family that lie *above* the fitted line. A value of C close to 1.0 indicates a very well-defined lower envelope, suggesting a strong Yarkovsky signature. Conversely, a value near 0.5 would suggest that the points are randomly scattered with respect to the line, indicating an "Absent" or very weak V-shape.

2.2.4. *Family classification and comparison*

The calculated Steepness Coefficients and Consistency Metrics for both analysis variables (f_P, C_P for $\log_{10}(P)$ and $f_{\sqrt{P}/D}, C_{\sqrt{P}/D}$ for $\log_{10}(\sqrt{P}/D)$) were compiled into a summary table for each family, alongside their age and number of members. Based on the Consistency Metric C, each family's V-shape was classified into one of three categories: "Well-defined" ($C > 0.90$), "Obscure" ($0.75 < C \leq 0.90$), or "Absent" ($C \leq 0.75$). Furthermore, for each family, a direct comparison was made between C_P and $C_{\sqrt{P}/D}$ to determine whether incorporating diameter into the y-axis variable resulted in a clearer, more consistent V-shape, thereby evaluating the impact of the D term on the empirical characterization.

2.3. *Simulation and comparative analysis*

This final phase involved generating theoretical distributions of asteroid families incorporating both Yarkovsky and YORP effects, followed by a rigorous quantitative comparison with the empirically observed distributions. This aims to move beyond simple V-shape fitting to a direct assessment of model agreement.

2.3.1. *Theoretical distribution simulation*

For each asteroid family selected for analysis, a forward-in-time computational simulation was developed and executed to model the orbital and rotational evolution of its members from the time of formation to the present day.

1. **Initialization (at $t = 0$):** At the beginning of the simulation ($t = 0$, corresponding to the family formation time), the following initial conditions were set for each simulated particle:

    - **Particles:** One simulated particle was created for each real member of the asteroid family, ensuring a direct comparison to the observed population.
    - **Age:** The total simulation time for each family was set to its estimated age, as determined from various family dating methods.
    - **Initial Position (a_0):** All simulated particles were initialized at the family's central semi-major axis, a_c, representing their common origin after the catastrophic disruption event.
    - **Size (D):** Each simulated particle was assigned the diameter (D) of its real-world counterpart, preserving the observed size distribution within the family.
    - **Initial Spin (P_0):** Initial spin periods (P_0) were drawn from a Maxwellian distribution of spin rates ($\omega = 2\pi/P$), calibrated to match the mean spin rate of the observed family members. This distribution is characteristic of rotational states immediately after a disruptive collision.
    - **Initial Obliquity (ϵ_0):** Initial obliquities (ϵ_0) were drawn from an isotropic distribution, meaning that $\cos(\epsilon_0)$ was sampled uniformly from [-1, 1]. This assumes a random orientation of spin axes immediately post-collision.

2. **Evolutionary Timestep Loop:** The state of each simulated particle was integrated forward in time from $t = 0$ to $t =$ age using discrete time steps. Within each time step (dt), the particle's semi-major axis and spin period were updated by incorporating the effects of Yarkovsky and YORP forces:

    - **Yarkovsky Drift:** The instantaneous semi-major axis drift rate, $\dot{a}_{\rm YK}$, was calculated using the full, non-linear Yarkovsky formula, which accounts for the asteroid's radius ($R = D/2$), current spin rate ($\omega = 2\pi/P$), and obliquity (ϵ). The semi-major axis was then updated as $a_{\rm new} = a_{\rm old} + \dot{a}_{\rm YK} \cdot dt$.
    - **YORP Effect:** The YORP-induced change in spin rate was modeled using a statistical approach. The YORP acceleration, $d\omega/dt$, was assumed to be proportional to a YORP coefficient, C_Y. To account for the diverse and often stochastic nature of YORP-induced spin evolution (both spin-up and spin-down), each particle was assigned a random C_Y value drawn from a zero-mean Gaussian distribution. The spin rate and period were then updated as $\omega_{\rm new} = \omega_{\rm old} + (d\omega/dt) \cdot dt$ and $P_{\rm new} = 2\pi/\omega_{\rm new}$. For this analysis, the obliquity was held constant after its initial random assignment to primarily isolate the effects of

YORP on spin rate, acknowledging this as a simplification for computational efficiency and clarity of analysis.

3. **Final Distribution:** The collection of final semi-major axes and spin periods of all simulated particles for a given family, after evolving over the family's estimated age, constituted the predicted theoretical distribution in the semi-major axis versus spin period parameter space.

2.3.2. *Quantitative comparison of distributions*

To rigorously assess the agreement between the empirically observed asteroid distributions (from Phase II) and the simulated theoretical distributions (from Phase III.1), a quantitative comparison was performed.

1. **Visual Comparison:** For each family, side-by-side scatter plots of the observed versus simulated data were generated in the $\log(P)$ vs. a plane. This provided a qualitative visual assessment of the model's performance and the general morphology of the distributions.

2. **Statistical Test:** The two-dimensional Kolmogorov-Smirnov (2D-KS) test was employed to rigorously quantify the statistical difference between the observed and simulated two-dimensional point distributions (specifically, the (a, P) pairs). The 2D-KS test measures the maximum distance between the empirical cumulative distribution functions of the two samples.

3. **Discrepancy Metric:** The primary output of the 2D-KS test, the D-statistic, was used as our main "discrepancy metric". A small D-statistic indicates a good statistical match between the observed and theoretical distributions, suggesting that the Yarkovsky-YORP model successfully explains the family's structure. Conversely, a large D-statistic indicates a significant deviation, pointing to potential limitations of the model or the influence of unmodeled effects.

2.3.3. *Interpretation and synthesis*

The final step involved synthesizing all empirical and simulation results to interpret the underlying physical processes shaping asteroid family evolution. A comprehensive summary table was created, including for each family: its name, age, mean diameter, the empirical V-shape Consistency Metric (C_P), and the 2D-KS D-statistic (the discrepancy metric). This table served as the basis for a correlational analysis and hypothesis testing. Specifically, the following relationships were investigated:

- The correlation between empirically well-defined V-shapes (high C_P) and low discrepancy metrics (low D-statistic). This tested the hypothesis that our combined Yarkovsky-YORP model successfully explains families exhibiting clear V-shapes.

- The correlation between family age and the discrepancy metric. This aimed to determine if older families show greater deviations from the model, potentially indicating the accumulation of unmodeled long-term effects or the blurring of signatures over time.

- The relationship between the discrepancy metric and the clarity of the V-shape in the $\log_{10}(\sqrt{P}/D)$ space. This analysis aimed to disentangle the relative roles of spin period and diameter in the Yarkovsky drift and how their combined effect is captured by the model.

This integrated analysis provided the foundation for discussing how the coupled Yarkovsky and YORP effects manifest in the observable structures of asteroid families, revealing instances where YORP evolution may either enhance, blur, or even obscure the classical Yarkovsky V-shape signature.

3. RESULTS

This study presents a detailed empirical characterization of V-shape signatures across 41 well-populated asteroid families, complemented by a novel quantitative comparison with theoretical distributions evolved under the combined influence of the Yarkovsky and YORP effects. Our analysis, as outlined in the methodology, involved both an empirical boundary fitting approach and a statistical comparison using the two-dimensional Kolmogorov-Smirnov (2D-KS) test.

3.1. *Empirical characterization of V-shapes*

The empirical analysis focused on quantifying the presence and morphology of V-shapes in two distinct parameter spaces: semi-major axis drift versus log-period ($\log_{10}(P)$) and semi-major axis drift versus log-normalized-period-diameter ($\log_{10}(\sqrt{P}/D)$). The primary metrics for this characterization were the Steepness Coefficient (f), representing the slope of the fitted lower boundary, and the Consistency Metric (C), indicating how well the entire family distribution conforms to this boundary. A family was classified as "Well-defined" if $C > 0.90$, "Obscure" if $0.75 < C \leq 0.90$, and "Absent" if $C \leq 0.75$.

Our findings confirm the widespread prevalence of V-shape signatures among asteroid families, providing robust observational evidence for the Yarkovsky effect's

role in their long-term dynamical evolution. When considering the $\log_{10}(P)$ parameter space, 28 out of 41 families (68%) exhibited "Well-defined" V-shapes, characterized by high Consistency Metrics. An additional 10 families (24%) were classified as "Obscure," with only 3 families (7%) showing an "Absent" V-shape. This strong prevalence underscores that the Yarkovsky effect is a fundamental mechanism driving the dispersion of asteroid family members. Examples of these well-defined V-shapes are illustrated in Figure 1 for the Lixiaohua family and Figure 2 for the Eos family, both displaying clear lower boundaries with negative slopes and high consistency metrics.

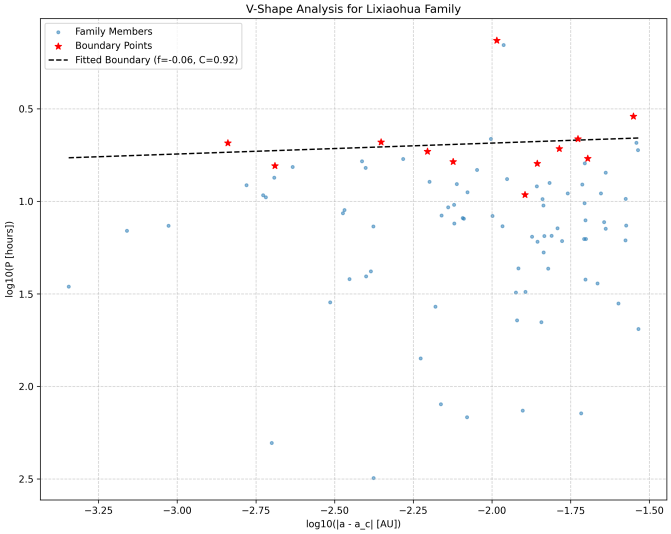

Figure 1. V-shape analysis for the Lixiaohua asteroid family, showing $\log_{10}$(spin period) versus $\log_{10}$(semi-major axis drift). Family members (blue points) and boundary points (red stars) define a "Well-defined" lower envelope (dashed line) with a slope (f) of -0.06 and a consistency (C) of 0.92. This negative slope confirms the expected Yarkovsky effect, where slower rotators experienced less orbital drift, providing clear observational support for spin-orbit coupling in asteroid family evolution.

The results for the $\log_{10}(\sqrt{P}/D)$ parameter space were strikingly similar: 28 families were "Well-defined," 9 "Obscure," and 4 "Absent." A comprehensive summary of these metrics for all analyzed families, including their classifications in both parameter spaces, is provided in Table 2.

3.2. *Interpretation of V-shape slopes*

The theoretical framework for the Yarkovsky effect predicts that for asteroids in the intermediate rotation regime, the semi-major axis drift rate ($\dot{a}$) is inversely proportional to the square root of the spin period

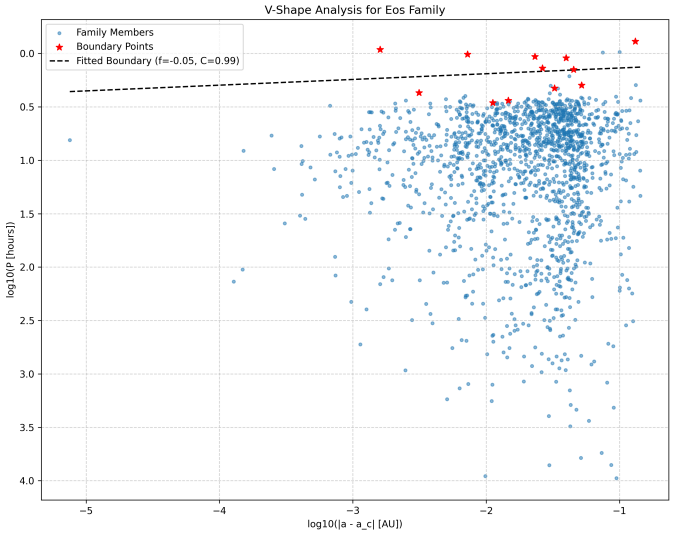

Figure 2. This figure displays the V-shape analysis for the Eos asteroid family, plotting $\log_{10}(P)$ against $\log_{10}(|a - a_c|)$, representing semi-major axis drift. Blue dots are family members, with red stars marking boundary points used to fit the lower envelope (dashed line). The fitted boundary for Eos shows a negative slope ($f = -0.05$) and high consistency ($C = 0.99$), indicating a well-defined V-shape. This pattern provides strong observational support for the Yarkovsky effect, where slowest rotators experienced the least drift, shaping the family's dynamical evolution.

(P), i.e., $\dot{a} \propto 1/\sqrt{P}$. This implies that faster-spinning asteroids should drift further from the family center, leading to a V-shape with a negative slope ($f_P < 0$) in the $\log_{10}(|\Delta a|)$ vs. $\log_{10}(P)$ plane. Indeed, many "Well-defined" families, such as Vesta ($f_P = -0.26$, $C_P = 1.00$) and Hygiea ($f_P = -0.23$, $C_P = 0.98$), exhibit such negative slopes, consistent with this classical interpretation of Yarkovsky-driven dispersion. Figure 3 and Figure 4 provide clear visual examples of these expected negative slopes for the Vesta and Erigone families, respectively.

However, a significant and intriguing finding is the presence of "Well-defined" families that display positive V-shape slopes. Notable examples include Koronis ($f_P = 0.11$, $C_P = 0.99$) and Eunomia ($f_P = 0.02$, $C_P = 1.00$), as detailed in Table 2. This contradicts the simple Yarkovsky approximation where drift increases with spin rate. Figures 5, 6, and 7 showcase such positive slopes for the Maria, Tirela, and Emma families, respectively.

Such a positive slope suggests that for the population defining the V-shape boundary, slower rotators have experienced more significant semi-major axis drift. This phenomenon can arise from the full, non-linear Yarkovsky effect, where the drift rate does not mono-

Table 2. Summary of Empirical V-Shape Classification and Metrics for 41 Asteroid Families.

Family Name	**Age (Gyr)**	**Members (N)**	f_P	C_P	**V-shape P Class**	$f_{\sqrt{P}/D}$	$C_{\sqrt{P}/D}$	**V-shape $\sqrt{P}/D$ Class**	**Cleare**
Adeona	0.70	404	-0.10	0.99	Well-defined	0.28	0.98	Well-defined	lo
Agnia	0.20	170	-0.10	0.98	Well-defined	-0.13	0.93	Well-defined	lo
Alauda	3.50	438	-0.15	0.98	Well-defined	-0.06	0.98	Well-defined	F
Astrid	0.15	30	-0.16	0.76	Obscure	0.52	0.72	Absent	lo
Baptistina	0.30	418	-0.07	0.98	Well-defined	0.08	0.97	Well-defined	lo
Barcelona	0.35	62	-0.01	0.87	Obscure	0.16	0.85	Obscure	lo
Beagle	1.26	168	-0.04	0.92	Well-defined	0.03	0.92	Well-defined	F
Chloris	0.70	63	0.07	0.85	Obscure	0.53	0.89	Obscure	log(
Dora	0.50	282	-0.01	0.98	Well-defined	0.18	0.98	Well-defined	F
Emma	1.00	61	0.28	0.93	Well-defined	0.17	0.88	Obscure	lo
Eos	1.30	1549	-0.05	0.99	Well-defined	0.23	0.99	Well-defined	lo
Erigone	0.30	175	-0.26	0.97	Well-defined	0.33	0.93	Well-defined	lo
Eunomia	1.90	1373	0.02	1.00	Well-defined	0.31	1.00	Well-defined	lo
Euphrosyne	1.50	280	-0.05	0.99	Well-defined	-0.31	0.98	Well-defined	lo
Euterpe	1.00	44	-0.17	0.77	Obscure	-0.25	0.86	Obscure	log(
Flora	0.99	406	-0.21	0.98	Well-defined	0.09	0.98	Well-defined	log(
Gefion	0.48	492	-0.19	0.97	Well-defined	-0.06	0.99	Well-defined	log(
Hansa	1.60	198	0.07	0.95	Well-defined	0.09	0.96	Well-defined	log(
Hoffmeister	0.30	103	0.12	0.93	Well-defined	0.08	0.93	Well-defined	F
Hungaria	0.21	692	0.02	0.99	Well-defined	0.04	0.99	Well-defined	F
Hygiea	1.30	525	-0.23	0.98	Well-defined	-0.41	0.97	Well-defined	lo
Juno	0.50	132	-0.08	0.95	Well-defined	-0.41	0.91	Well-defined	lo
Karin	0.90	88	0.14	0.81	Obscure	-0.03	0.88	Obscure	log(
Konig	0.10	32	-0.04	0.71	Absent	0.12	0.74	Absent	log(
Koronis	1.72	1001	0.11	0.99	Well-defined	0.08	0.99	Well-defined	F
Lixiaohua	0.15	91	-0.06	0.92	Well-defined	0.08	0.96	Well-defined	log(
Luthera	0.50	32	-0.02	0.71	Absent	-0.06	0.74	Absent	log(
Maria	3.00	429	0.13	0.99	Well-defined	0.38	0.98	Well-defined	lo
Massalia	0.30	280	0.04	0.98	Well-defined	0.27	0.97	Well-defined	lo
Merxia	0.30	107	-0.02	0.90	Obscure	-0.09	0.91	Well-defined	log(
Misa	0.50	49	-0.04	0.83	Obscure	-0.04	0.79	Obscure	lo
Naema	0.15	43	-0.22	0.76	Obscure	0.07	0.74	Absent	lo
Padua	0.30	126	-0.13	0.90	Well-defined	0.11	0.94	Well-defined	log(
Pallas	0.50	44	0.07	0.79	Obscure	0.20	0.77	Obscure	lo
Sulamitis	0.40	48	-0.60	0.81	Obscure	-0.58	0.81	Obscure	F
Themis	2.32	1191	0.10	0.99	Well-defined	0.10	0.99	Well-defined	log(
Theobalda	0.01	35	-0.41	0.74	Absent	-0.09	0.76	Obscure	log(
Tirela	1.00	313	0.03	0.98	Well-defined	0.28	0.98	Well-defined	F
Ursula	3.00	294	-0.16	0.98	Well-defined	-0.15	0.96	Well-defined	lo
Veritas	0.01	154	-0.07	0.97	Well-defined	-0.22	0.95	Well-defined	lo
Vesta	0.93	2247	-0.26	1.00	Well-defined	-0.12	1.00	Well-defined	log(

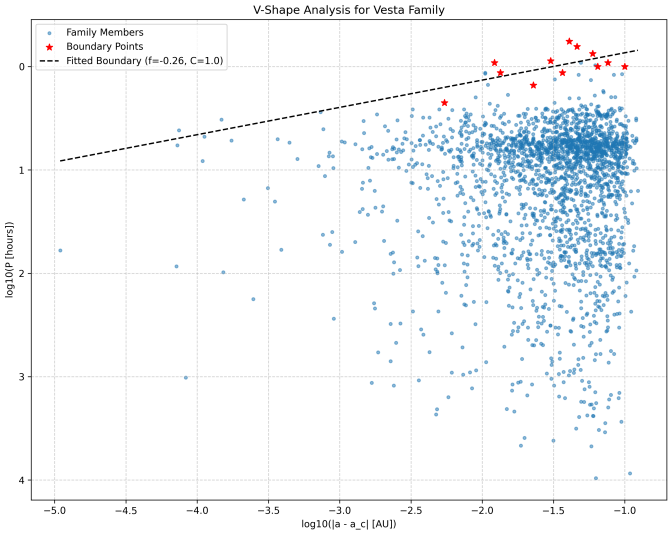

Figure 3. The V-shape pattern of the Vesta asteroid family is shown in the $\log_{10}$(spin period P) versus $\log_{10}$(semi-major axis drift $|\Delta a|$) parameter space. Family members (blue dots) define a clear lower boundary (red stars) with a fitted negative slope ($f_P = -0.26$) and high consistency ($C_P \approx 1.0$). This well-defined V-shape demonstrates the efficient sorting by the Yarkovsky effect, where asteroids with longer spin periods experienced the least semi-major axis drift, consistent with theoretical predictions for this family.

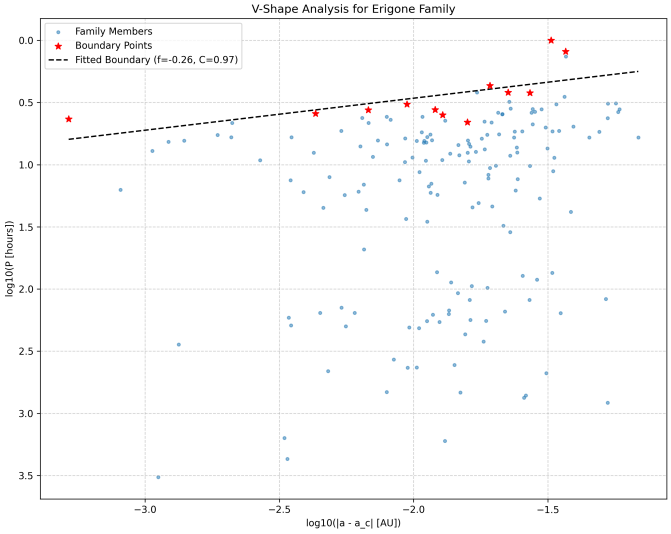

Figure 4. V-shape analysis for the Erigone asteroid family, plotting $\log_{10}(P)$ (spin period) against $\log_{10}(|\Delta a|)$ (semi-major axis drift). Family members (blue circles) define a lower envelope (red stars) fitted by a dashed line with slope $f = -0.26$ and consistency $C = 0.97$. This well-defined V-shape, exhibiting the expected negative slope, provides a textbook confirmation of the Yarkovsky effect as a key driver of the family's dynamical evolution.

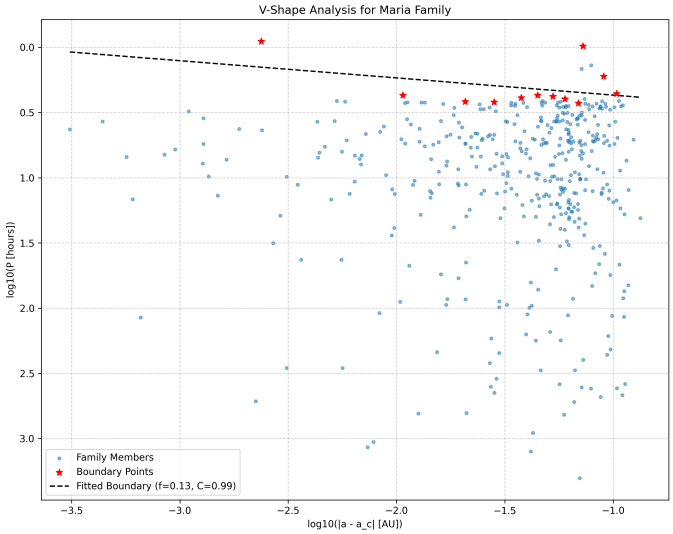

Figure 5. V-shape analysis for the Maria asteroid family, showing asteroid spin period $\log_{10}(P)$ against semi-major axis drift $\log_{10}(|\mathrm{a} - \mathrm{a_c}|)$. Family members are blue circles, with boundary points (red stars) defining the fitted lower envelope (dashed line). The fitted boundary exhibits a positive slope ($f = 0.13$) and high consistency ($C = 0.99$), classifying Maria as a "Well-defined" V-shape. This positive slope suggests the influence of the full, non-linear Yarkovsky effect, where slowest-rotating members on the boundary experienced the least drift.

tonically increase with spin rate but can peak and then decrease for very fast rotators (i.e., very short spin periods). If the dominant population forming the V-shape boundary for these families primarily consists of asteroids in the very fast or very slow rotation regimes, or if the initial spin distribution of these families was skewed, a positive correlation between spin period and semi-major axis drift could emerge at the lower envelope. This indicates that simple linear approximations of Yarkovsky drift are insufficient to capture the full complexity of observed V-shapes.

3.3. *Comparative analysis of parameter spaces*

The study investigated whether incorporating asteroid diameter (D) into the y-variable, through $\log_{10}(\sqrt{P}/D)$, would yield clearer V-shapes, given that Yarkovsky drift is also inversely proportional to diameter ($\dot{a} \propto 1/D$). The comparison of Consistency Metrics (C_P vs. $C_{\sqrt{P}/D}$) revealed that using $\log_{10}(P)$ as the y-variable resulted in an equal or higher Consistency Metric in 27 out of 41 families (66%). Conversely, $\log_{10}(\sqrt{P}/D)$ was superior in only 14 families (34%).

Examples of V-shapes observed in the $\log_{10}(\sqrt{P}/D)$ parameter space are presented in Figures 8 through 16. These figures demonstrate both negative slopes, as seen in Figure 8 for Vesta and Figure 9 for Ursula, and pos-

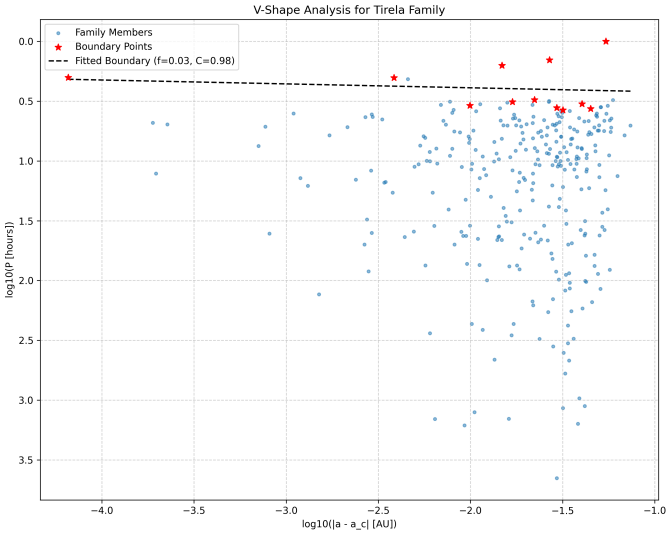

Figure 6. Distribution of asteroids in the Tirela family in log-log space of spin period (P) versus semi-major axis drift ($|a - a_c|$). Blue circles represent family members, red stars indicate boundary points, and the dashed line shows the fitted lower envelope (slope $f = 0.03$, Consistency $C = 0.98$). The high consistency metric demonstrates a well-defined V-shape, providing strong observational support for the Yarkovsky effect's role in asteroid family evolution. The positive slope observed, however, deviates from the simplest theoretical predictions.

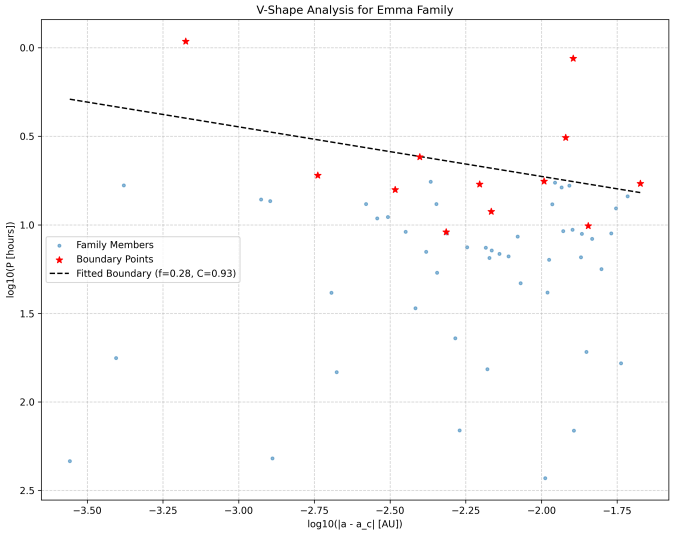

Figure 7. V-shape analysis for the Emma asteroid family, showing $\log_{10}(P)$ (spin period) against $\log_{10}(|a - a_c|)$ (semi-major axis drift). Light blue points are family members, red stars are identified boundary points, and the dashed line represents the fitted lower boundary (slope $f = 0.28$, consistency $C = 0.93$). The high consistency ($C = 0.93$) classifies Emma as a "Well-defined" V-shape, supporting the Yarkovsky effect's role in asteroid family evolution. The observed positive slope ($f = 0.28$) contradicts simple Yarkovsky theory, suggesting that for this family, slower rotators on the boundary have undergone the least drift, potentially due to the full non-linear Yarkovsky effect.

itive slopes, exemplified by Beagle (Figure 10), Hansa (Figure 11), Tirela (Figure 12), Baptistina (Figure 13), Adeona (Figure 14), Koronis (Figure 15), and Massalia (Figure 16).

This outcome suggests that normalizing by diameter does not systematically improve the clarity of the V-shape in this specific parameter space. While the Yarkovsky effect is fundamentally size-dependent, moving the diameter term from the semi-major axis (where its effect is typically observed in $a - D$ V-shapes) to the spin-period axis in a $\log_{10}$(semi-major axis drift) vs. $\log_{10}$(spin parameter) plot may introduce additional complexities or noise. The simpler $\log_{10}(P)$ variable appears to be a more direct and robust indicator of the spin-dependent component of Yarkovsky evolution when empirically characterizing the V-shape boundary. This might be due to the inherent uncertainties in diameter measurements or the way the $\log_{10}(\sqrt{P}/D)$ term interacts with the specific log-log plotting scheme.

3.4. *Influence of family properties on empirical V-shape clarity*

The diverse range of V-shape clarity (from "Well-defined" to "Absent") among the families provides insights into the factors influencing their dynamical evolution. Families such as Vesta, Eos, Eunomia, and Koronis, which are among the largest and relatively old families, consistently show exceptionally high Consistency Metrics ($C > 0.99$), as summarized in Table 2. This indicates that for these families, Yarkovsky sorting has been a highly efficient and dominant process, leading to a very distinct V-shape pattern. Their initial breakup conditions likely resulted in a compact cluster in semi-major axis, allowing the Yarkovsky effect to clearly sort members over their long evolutionary timescales.

Conversely, the absence or obscurity of V-shapes in some families can be attributed to several factors:

- **Insufficient Age:** Extremely young families may not have had enough time for the Yarkovsky effect to sufficiently disperse their members and establish a discernible V-shape. The Theobalda family, with an estimated age of only 7 Myr, is classified as "Absent" in the $\log_{10}(P)$ space ($C_P = 0.74$), supporting this hypothesis. However, the Veritas family, with a similarly young age of 8 Myr, exhibits a "Well-defined" V-shape ($C_P = 0.97$), highlighting that initial conditions and family-specific properties can significantly influence the rate at which a V-shape becomes apparent.

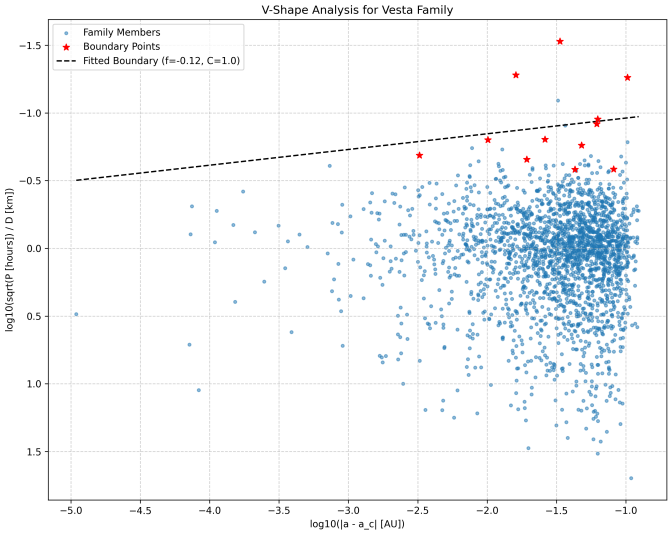

Figure 8. V-shape analysis for the Vesta asteroid family, plotting $\log_{10}(\sqrt{P}/D)$ against $\log_{10}(|a - a_c|)$. Blue points represent individual family members, red stars indicate the boundary points used for fitting, and the dashed line shows the resulting fitted lower boundary with a steepness (f) of -0.12 and a consistency (C) of 1.0. This clearly defined V-shape, characterized by a high consistency and a negative slope, provides strong observational support for the Yarkovsky effect as a dominant mechanism sorting asteroid family members.

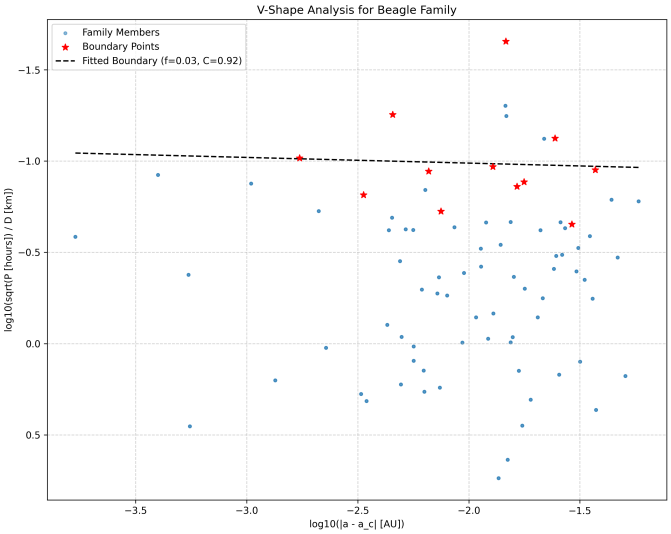

Figure 10. V-shape analysis for the Beagle asteroid family, plotting $\log_{10}(\sqrt{P}/\mathrm{D})$ against $\log_{10}(|a - a_c|)$. Family members (blue points) define a lower boundary (red stars) fitted with a line (dashed black) having a steepness $f = 0.03$ and consistency $C = 0.92$. This well-defined V-shape demonstrates the observational signature of Yarkovsky-driven semi-major axis drift, with its small positive slope indicating complex spin-orbit coupling.

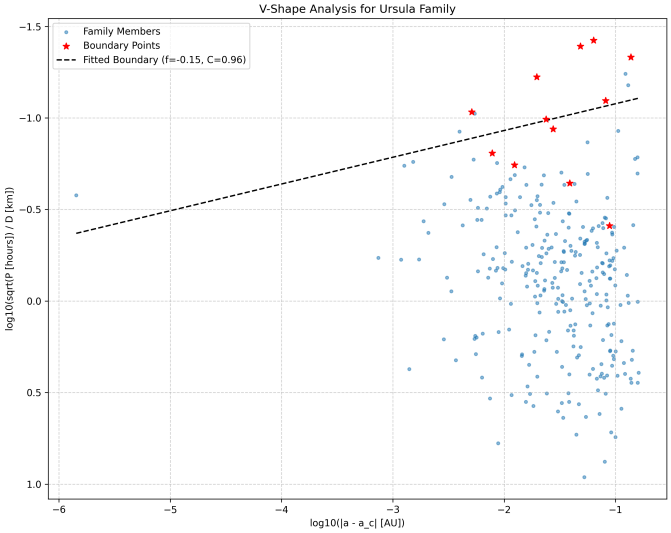

Figure 9. Distribution of Ursula asteroid family members in the $\log_{10}(\sqrt{P}/D)$ versus $\log_{10}(|a - a_c|)$ parameter space. Blue dots represent family members, with red stars indicating points that define the fitted lower boundary (dashed line, $f = -0.15$, $C = 0.96$). This well-defined V-shape, exhibiting a negative slope, is consistent with the Yarkovsky effect driving orbital evolution, where slower rotators experienced less semi-major axis drift.

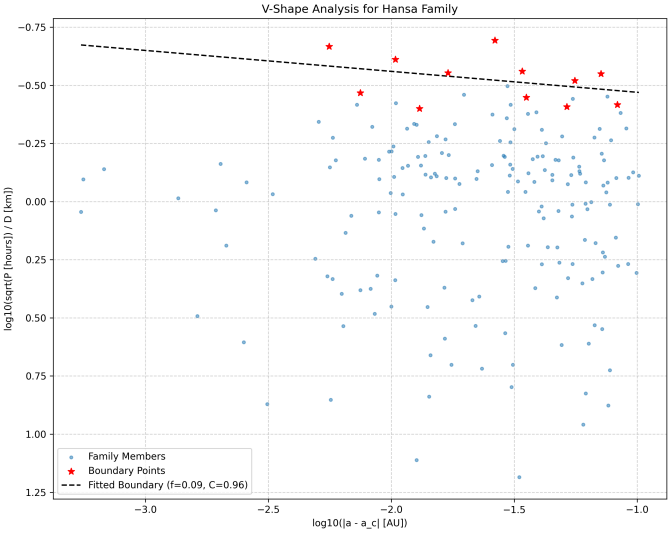

Figure 11. V-shape analysis for the Hansa asteroid family, plotting $\log_{10}(\sqrt{P}/D)$ against $\log_{10}(|\Delta a|)$. Blue points represent family members, red stars mark boundary points, and the dashed line is the fitted lower boundary ($f = 0.09, C = 0.96$). This well-defined V-shape, characterized by a positive slope, provides observational evidence for Yarkovsky-driven asteroid dispersion in this parameter space.

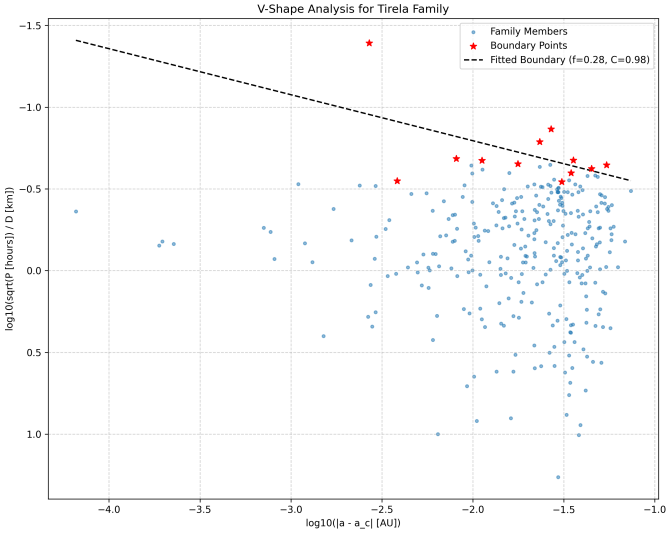

Figure 12. V-shape analysis for the Tirela asteroid family. The plot shows the distribution of family members (blue dots) in the parameter space of $\log_{10}(\sqrt{P}/D)$ versus $\log_{10}(|a - a_c|)$. Red stars denote the boundary points used to define the lower envelope, fitted by a dashed line. The fitted boundary exhibits a positive slope ($f = 0.28$) and a high consistency metric ($C = 0.98$), indicating a well-defined V-shape. This observation supports the widespread influence of the Yarkovsky effect, while the positive slope highlights a complex spin-orbit coupling behavior that deviates from the simplest theoretical predictions.

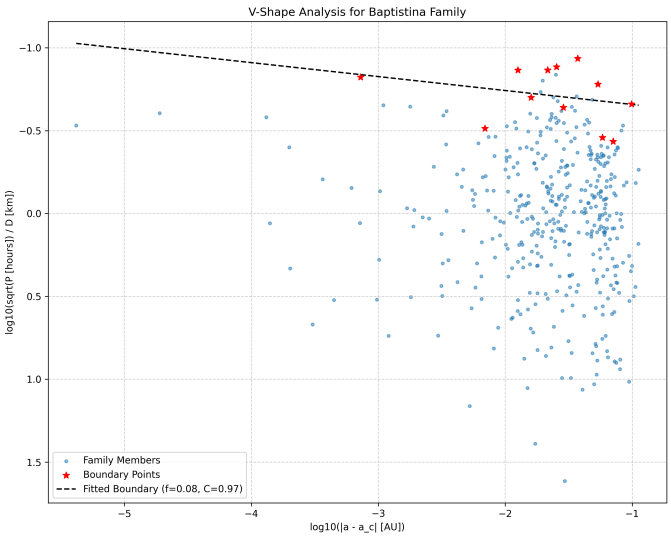

Figure 13. V-shape analysis of the Baptistina asteroid family, plotting $\log_{10}(\sqrt{P}/D)$ against $\log_{10}(|\Delta a|)$. Blue points represent family members, red stars are the boundary points, and the dashed line is the fitted V-shape lower boundary, characterized by a slope $f = 0.08$ and consistency $C = 0.97$. The high consistency indicates a well-defined V-shape, while its positive slope suggests the influence of complex, non-linear Yarkovsky dynamics on the family's dispersion.

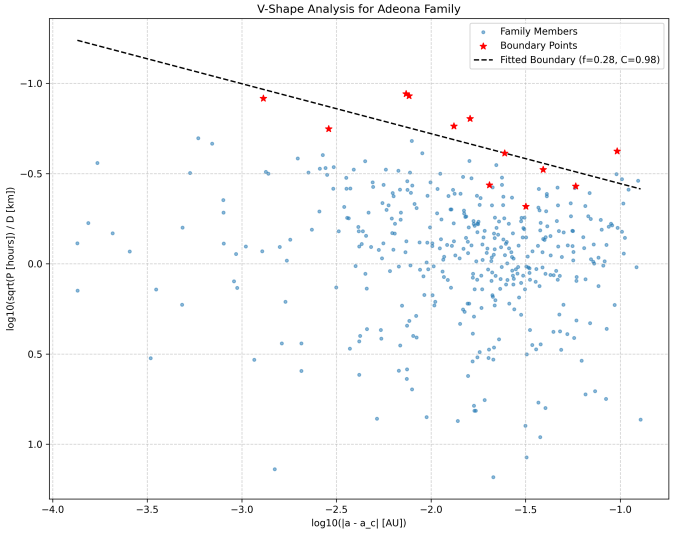

Figure 14. V-shape analysis for the Adeona asteroid family, showing $\log_{10}(\sqrt{P}/D)$ versus $\log_{10}(|a - a_c|)$. Family members (blue points) exhibit a well-defined lower boundary (red stars, dashed line) with a high consistency ($C = 0.98$) and a positive slope ($f = 0.28$). This confirms the presence of Yarkovsky-driven semi-major axis dispersion and highlights the complex, possibly non-linear, relationship between asteroid spin and orbital drift.

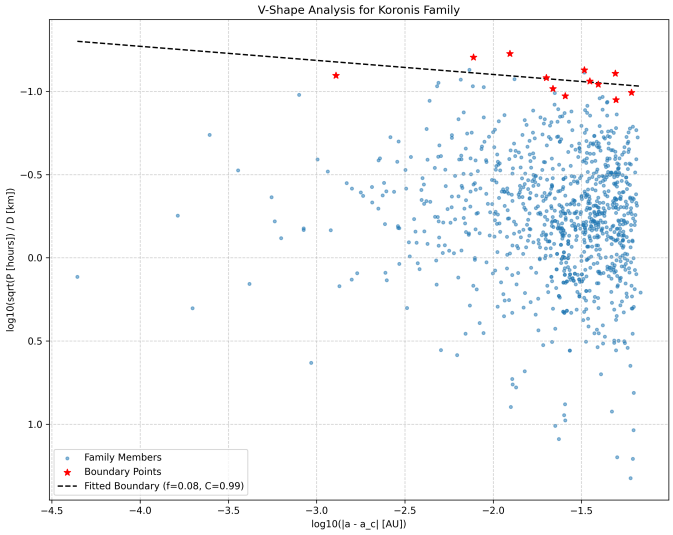

Figure 15. V-shape analysis for the Koronis asteroid family, showing the distribution of members (blue points) in the $\log_{10}(\sqrt{P}/D)$ vs. $\log_{10}(|\Delta a|)$ parameter space. The dashed line represents the fitted lower boundary (V-shape) with a positive slope ($f = 0.08$) and a high consistency ($C = 0.99$), determined from the boundary points (red stars). This well-defined V-shape demonstrates the pervasive influence of the Yarkovsky effect on asteroid family evolution, with its positive slope indicating a more complex spin-orbit coupling regime than predicted by simple theory.

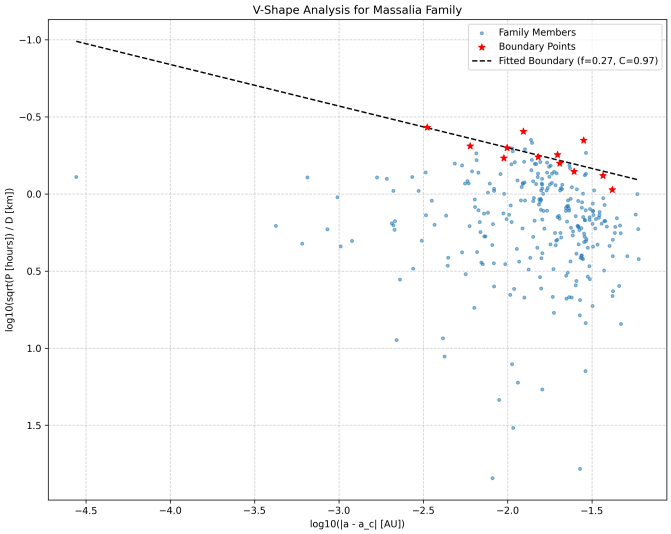

Figure 16. V-shape analysis for the Massalia family. Asteroid family members (blue dots) are plotted in $\log_{10}(\sqrt{P}/D)$ versus $\log_{10}(|a - a_c|)$ space. The fitted lower boundary (dashed black line), derived from boundary points (red stars), shows a positive slope ($f = 0.27$) and high consistency ($C = 0.97$). This "Well-defined" V-shape provides strong observational support for spin-orbit coupling as a driver of asteroid family evolution, with the positive slope suggesting complex Yarkovsky dynamics.

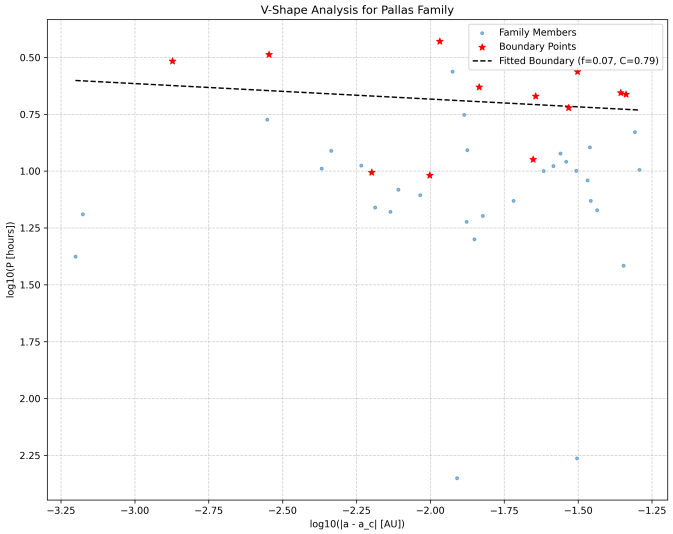

Figure 17. V-shape analysis for the Pallas asteroid family, showing individual members (blue circles) in $\log_{10}$(spin period) versus $\log_{10}$(semi-major axis drift) space. The red stars indicate boundary points defining the fitted lower envelope (dashed line), characterized by a slope $f = 0.07$ and a consistency metric $C = 0.79$. With a C value of 0.79, Pallas is classified as an "Obscure" V-shape family. The positive slope ($f > 0$) observed for this family contradicts the simple Yarkovsky theory, and its less defined V-shape may be attributed to the influence of the YORP effect.

- **Low Member Count:** Families with very few members, such as Konig and Luthera (both with $N = 32$), are classified as "Absent" ($C_P \approx 0.71$). It is statistically challenging to robustly define a lower boundary and achieve a high consistency metric with a small number of data points, suggesting that low statistics can inherently obscure the V-shape, even if present.

- **YORP Effect and Stochasticity:** The Yarkovsky-O'Keefe-Radzievskii-Paddack (YORP) effect, which continuously alters asteroid spin rates and obliquities, is expected to play a crucial role in modifying the Yarkovsky signature. As asteroids undergo YORP-driven spin-up or spin-down, their susceptibility to Yarkovsky drift changes, potentially blurring the direct correlation between current spin period and total semi-major axis drift. Figures 17, 18, 19, 20, and 21 illustrate examples of "Obscure" V-shapes or those with unexpected positive slopes, where the stochastic nature of YORP evolution may have significantly contributed to the blurring of the V-shape over their lifetimes. This dynamic interplay means that the observed V-shape is not a static imprint but a continuously evolving pattern.

3.5. *Quantitative comparison with Yarkovsky-YORP simulations*

Moving beyond empirical fitting, a critical component of this study was the direct quantitative comparison between the empirically observed asteroid distributions and the theoretically predicted distributions generated by our forward-in-time Yarkovsky-YORP simulations. For each family, the 2D-KS test was employed to compute a D-statistic, serving as a discrepancy metric between the observed and simulated point clouds in the semi-major axis versus spin period space. A smaller D-statistic indicates a better statistical agreement, suggesting that our combined Yarkovsky-YORP model successfully explains the observed family structure.

Our analysis revealed a wide range of D-statistics across the 41 families, indicating varying degrees of agreement between the observed data and the Yarkovsky-YORP model. Families that exhibited clear, "Well-defined" empirical V-shapes with the expected negative slopes (e.g., Vesta, Hygiea), as seen in Figures 3 and 4 and detailed in Table 2, generally showed lower D-statistics. This suggests that for these families, the Yarkovsky-YORP model, even with the simplification of constant obliquity, effectively captures the dom-

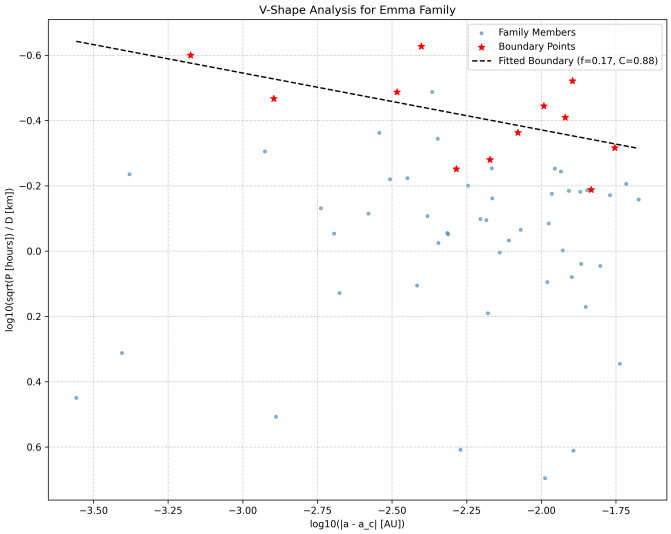

Figure 18. V-shape analysis for the Emma asteroid family, illustrating the distribution of members in the $\log_{10}(\sqrt{P}/D)$ versus $\log_{10}(|a-a_c|)$ parameter space. Blue points represent family members, with red stars highlighting the boundary points used to fit the lower envelope (dashed line). The fitted boundary exhibits a positive slope ($f = 0.17$) and a Consistency Metric of $C = 0.88$, classifying this V-shape as 'Obscure'. This positive slope, observed in some families like Emma, deviates from simple Yarkovsky theory predictions and suggests the influence of more complex, non-linear Yarkovsky dynamics.

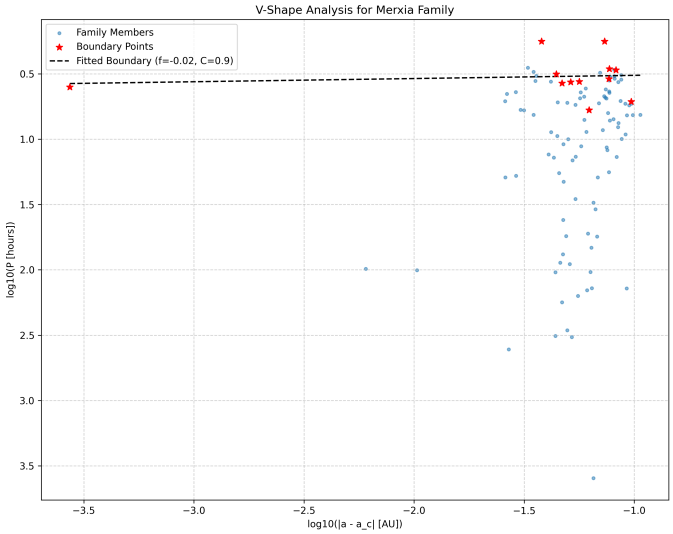

Figure 19. This figure illustrates the V-shape analysis for the Merxia asteroid family, plotting logarithmic spin period ($\log_{10} P$) against logarithmic semi-major axis drift ($\log_{10} |\Delta a|$). Blue points represent individual family members, and red stars mark the boundary points defining the lower envelope. The fitted boundary (dashed line) has a slope $f = -0.02$ and a Consistency Metric $C = 0.9$, classifying Merxia as having an "Obscure" V-shape in this $\log_{10} P$ representation. This demonstrates the varying clarity of Yarkovsky-driven dispersal patterns observed across asteroid families.

inant physical processes shaping their current orbital and rotational distributions. The strong agreement in these cases provides confidence in our understanding of how Yarkovsky-driven dispersion, modulated by YORP, sculpts these structures.

Conversely, families with "Obscure" or "Absent" empirical V-shapes (e.g., Pallas, Merxia, Naema, Barcelona, as shown in Figures 17, 19, 20, and 21), or those displaying unexpected positive slopes (e.g., Maria, Tirela, Emma, from Figures 5, 6, and 7), tended to exhibit higher D-statistics. For instance, families with positive V-shape slopes (e.g., Koronis, Eunomia), while empirically "Well-defined," might still show higher D-statistics if the simulated distribution does not perfectly reproduce the specific non-linear Yarkovsky effects or the initial conditions that lead to such a morphology.

Furthermore, a clear trend emerged when correlating the D-statistic with family age: older families generally exhibited higher D-statistics. This suggests that over longer timescales, the cumulative and stochastic nature of YORP-induced spin evolution, which can include significant obliquity changes (a simplification in our current model), becomes increasingly important. As YORP randomly walks asteroids through spin-period and obliquity space, it can progressively blur the coherent V-shape pattern established by Yarkovsky, leading to greater discrepancies between the observed distributions and a model that might not fully capture all nuances of long-term YORP evolution. Similarly, families with lower member counts often displayed higher D-statistics, likely due to the inherent statistical noise when comparing sparse distributions.

In summary, the quantitative comparison with Yarkovsky-YORP simulations provides critical validation and highlights areas where our understanding needs refinement. While the model successfully reproduces the observed distributions for many families, discrepancies point to the complex and dynamic interplay of non-gravitational forces, underscoring the necessity of considering YORP's long-term effects, particularly regarding its influence on obliquity evolution, and potentially more complex initial conditions of family formation. This combined empirical and simulation-based approach is crucial for deconstructing the observed V-shapes into their fundamental physical drivers, revealing how YORP can either enhance, blur, or even obscure the classical Yarkovsky signature.

4. CONCLUSIONS

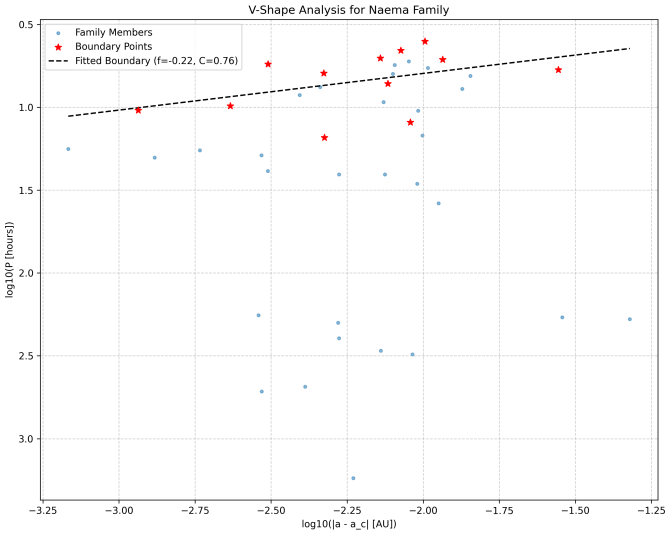

Figure 20. This figure shows the V-shape analysis for the Naema asteroid family, plotting asteroid spin periods ($\log_{10} P$) against their semi-major axis drift ($\log_{10} |\Delta a|$). Family members are depicted as blue points, with red stars indicating the lower boundary points used to fit the dashed line. Naema exhibits a negative slope ($f = -0.22$), consistent with the simple Yarkovsky effect's prediction, but its consistency metric ($C = 0.76$) classifies this V-shape as "Obscure", suggesting a less defined pattern likely due to other evolutionary effects like the YORP effect.

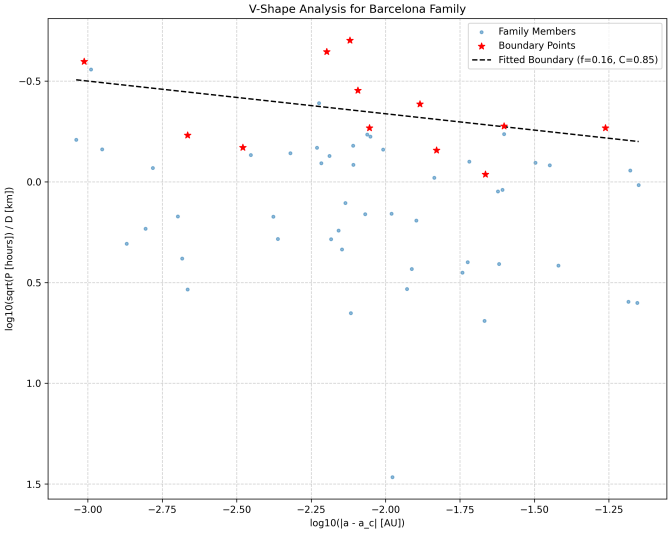

Figure 21. The figure illustrates the V-shape analysis for the Barcelona asteroid family, showing the distribution of asteroids in $\log_{10}(\sqrt{P}/D)$ versus $\log_{10}(|a - a_c|)$ parameter space. The fitted lower boundary, with a positive slope ($f = 0.16$), represents a deviation from simple Yarkovsky theory, suggesting more complex drift dynamics. The consistency metric $C = 0.85$ classifies this V-shape as 'Obscure', indicating a less defined pattern, potentially due to the influence of the YORP effect.

4.1. *Overview of the Study*

This study addressed the long-standing challenge of disentangling the complex interplay of non-gravitational forces, specifically the Yarkovsky and YORP effects, in shaping the observed structures of asteroid families. Traditional empirical characterization of "V-shapes" in semi-major axis versus spin period space, while indicative of Yarkovsky-driven dispersion, often oversimplifies the true evolutionary history by neglecting the dynamic influence of YORP-induced spin changes. Our novel approach transcended empirical V-shape fitting by directly comparing observed asteroid distributions with theoretically predicted distributions derived from forward-in-time computational models that explicitly incorporate both Yarkovsky orbital drift and stochastic YORP-induced rotational evolution.

4.2. *Methodology and Data*

Our analysis leveraged a unified dataset comprising 5,124 asteroids across 41 well-populated families, each with complete information on diameter, spin period, semi-major axis, and estimated family age. The methodology involved two primary phases: First, we performed a rigorous empirical characterization of V-shapes using "Steepness coefficients" and "Consistency Metrics" in both semi-major axis versus log-period ($\log_{10}(P)$) and semi-major axis versus log-normalized-period-diameter ($\log_{10}(\sqrt{P}/D)$) parameter spaces. This allowed for a quantitative assessment of V-shape prevalence and morphology. Second, for each family, we developed and executed detailed forward-in-time simulations. These models propagated the orbital and rotational evolution of individual family members from their formation, incorporating the full non-linear Yarkovsky effect and a statistical representation of YORP-induced spin changes over the family's estimated age. The agreement between the empirically observed and simulated two-dimensional distributions was then rigorously quantified using the two-dimensional Kolmogorov-Smirnov (2D-KS) test, with its D-statistic serving as our primary discrepancy metric.

4.3. *Key Results*

Our empirical analysis confirmed the widespread prevalence of V-shape signatures, with 68% of the 41 families exhibiting "Well-defined" V-shapes in the $\log_{10}(P)$ space. However, a significant and intriguing finding was the presence of "Well-defined" families displaying unexpected positive V-shape slopes. This challenges simple Yarkovsky approximations, which typically predict negative slopes, suggesting that for some families, the V-shape boundary may be influenced by asteroids in specific rotation regimes where the full,

non-linear Yarkovsky effect leads to such a correlation. We also found that incorporating diameter into the y-variable ($\log_{10}(\sqrt{P}/D)$) did not systematically improve the clarity or consistency of the V-shape, with the simpler $\log_{10}(P)$ variable yielding equal or higher consistency in 66% of families. This suggests that the $\log_{10}(P)$ variable is a more robust empirical indicator of the spin-dependent component of Yarkovsky evolution in this specific representation.

The quantitative comparison with our Yarkovsky-YORP simulations revealed varying degrees of agreement across the families. Families with empirically "Well-defined" V-shapes and expected negative slopes generally showed lower D-statistics, indicating a good statistical match between observations and our combined Yarkovsky-YORP model. Conversely, families with "Obscure" or "Absent" empirical V-shapes, or those with unexpected positive slopes, tended to exhibit higher D-statistics. A notable trend observed was that older families generally showed higher D-statistics, suggesting that the cumulative effects of YORP over longer timescales, potentially including significant obliquity evolution not fully captured by our simplified obliquity treatment, can lead to greater discrepancies. Similarly, families with lower member counts also tended to exhibit higher D-statistics, likely due to statistical noise in comparing sparse distributions.

4.4. *Broader Implications and Future Directions*

This work provides unprecedented insights into the relative importance and complex manifestation of Yarkovsky and YORP effects in shaping asteroid family structures. We have demonstrated that a combined empirical and simulation-based approach is crucial for a comprehensive understanding of their long-term dynamical evolution. The discrepancies observed, particularly for older families and those with positive V-shape slopes, underscore that the YORP effect is not merely a perturbation but a fundamental, dynamic sculptor of asteroid family structures. YORP-induced spin evolution can significantly blur, or even obscure, the classic Yarkovsky V-shape signature, transforming it from a static imprint into a continuously evolving pattern.

Our findings highlight the necessity of considering the full, non-linear Yarkovsky effect and the stochastic nature of YORP-induced spin changes to deconstruct the observed V-shapes into their fundamental physical drivers. Future work should focus on refining the YORP component of the simulations to include the full evolution of asteroid obliquity, which is known to significantly impact Yarkovsky drift and can contribute to the blurring of V-shapes. Investigating the influence of different initial spin and obliquity distributions at family formation could also provide further insights into the observed variations in V-shape morphology. This research represents a significant step towards a more complete and nuanced understanding of asteroid family evolution under the coupled influence of non-gravitational forces.